Journal of Radiation Research, Vol. 63, No. 2, 2022, pp. 221–229
https://doi.org/10.1093/jrr/rrab123
Advance Access Publication: 10 January 2022

Dose- and LET-dependent changes in mouse skin contracture up to a year after either single dose or fractionated doses of carbon ion or gamma rays

Koichi Ando[1,*], Yukari Yoshida[1], Ryoichi Hirayama[2], Sachiko Koike[2] and Naruhiro Matsufuji[2]

[1]Gunma University Heavy Ion Medical Center, Showa-machi 3-39-22, Maebashi-shi, Gunma, Japan 371-8511
[2]Institute for Quantum Medical Science, National Institutes for Quantum Science and Technology, Anagawa 4-9-1, Chiba, Japan 263-8555
*Corresponding author. Gunma University Heavy Ion Medical Center, Showa-machi 3-39-22, Maebashi0shi, Gunma, Japan 371-8511,
Email address: kando3@gunma-u.ac.jp
(Received 8 July 2021; revised 18 October 2021; editorial decision 10 December 2021)

ABSTRACT

Time dependence of relative biological effectiveness (RBE) of carbon ions for skin damage was investigated to answer the question of whether the flat distribution of biological doses within a Spread-Out Bragg peak (SOBP) which is designed based on *in vitro* cell kill could also be flat for *in vivo* late responding tissue. Two spots of Indian ink intracutaneously injected into the legs of C3H mice were measured by calipers. An equieffective dose to produce 30% skin contraction was calculated from a dose–response curve and used to calculate the RBE of carbon ion beams. We discovered skin contraction progressed after irradiation and then reached a stable/slow progression phase. Equieffective doses decreased with time and the decrease was most prominent for gamma rays and least prominent for 100 keV/μm carbon ions. Survival parameter of alpha but not beta in the linear-quadratic model is closely related to the RBE of carbon ions. Biological doses within the SOBP increased with time but their distribution was still flat up to 1 year after irradiation. The outcomes of skin contraction studies suggest that (i) despite the higher RBE for skin contracture after carbon ions compared to gamma rays, gamma rays can result in a more severe late effect of skin contracture. This is due to the carbon effect saturating at a lower dose than gamma rays, and (ii) the biological dose distribution throughout the SOBP remains approximately the same even one year after exposure.

Keywords: LET; RBE; fibrosis; Fe-Plot

INTRODUCTION

Carbon-ion radiotherapy (CIR) is cutting-edge technology in oncology and more effective than X-rays due to its physical property of high linear energy transfer (LET). Since 1994 when the National Institute of Radiological Sciences (NIRS) at Chiba in Japan started CIR, the number of patients worldwide who received CIR by 2019 has reached over 30 000 and this number continues to increase [1]. Different from X-rays but like proton beams, Bragg peaks of carbon-ions should be spread out and form a spread-out Bragg peak (SOBP) to irradiate a voluminous tumor. This causes LET and therefore relative biological effectiveness (RBE) gradient within the SOBP. The design of SOBP uses RBE values of *in vitro* cell-kill at NIRS, Japan [2, 3] and survival parameters of the linear-quadratic model in GSI Helmholzzentrum für Schwerionenforschung GmbH, Germany [4, 5]. We previously reported that the SOBP being used at Chiba provides flat biological dose distribution when early skin reaction was concerned [6]. However, the unanswered question yet to be solved is: does the SOBP currently used by CIR in the world provide flat biological-dose distribution for late normal tissue damage? We here answered this question by investigating RBE values of carbon ions for skin contraction as a surrogate endpoint of dermal fibrosis in mice. One of the most common adverse effects of radiotherapy is fibrosis which usually develops within 6–12 months after completion of therapy [7] in many organ systems including skin and lung [8]. Fibrosis involves chemical and biological processes such as inflammation and cytokine cascades and is developed by survived cells responding to these processes. This is different from early skin reaction and *in vitro* colony formation that does not depend on these environmental processes.

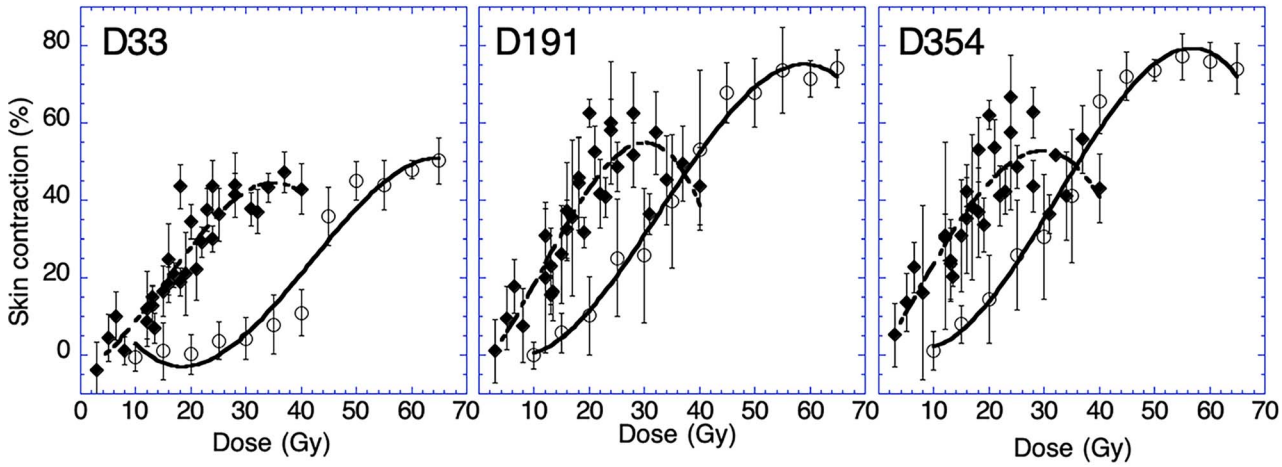

Fig. 1. Dose–response of skin contraction. Distance of two tattoo spots was measured by calipers after 33, 191 and 354 days after single doses of radiation. Skin contraction was calculated by comparing pre- and post-irradiation values in identical mice. Open circle (◯) is for gamma rays and closed diamond (♦) for 100 keV/μm carbon ions.

MATERIALS AND METHODS

Mice and radiation

C3H/HeMsNrsf female mice aged 12–18 weeks old were used for this study. The mice were produced and maintained in specific pathogen-free (SPF) facilities at the NIRS. A total of 2730 mice were used in these experiments. Five mice were used for all treated and control groups. The animals involved in these studies were procured, maintained and used under the Recommendations for Handling of Laboratory Animals for Biomedical Research, compiled by the Committee on the Safety and Handling Regulations for Laboratory Animal Experiments of NIRS. Mice irradiated with gamma rays were kept under SPF conditions while those with carbon ions were moved to conventional conditions.

Carbon-12 ions were accelerated by the Heavy Ion Medical Accelerator in Chiba (HIMAC) synchrotron up to 290 MeV/u [2]. With a dose rate of approximately 3 Gy/min, the LETs of carbon ions were 14 keV/μm at the entrance of a 6-cm SOBP and 100 keV/μm at the very end of the SOBP. An ionization-chamber method was adapted for the dosimetry of carbon ions. The W value of air for the carbon beam is assumed to be 35.2 eV, which is the same as that for high-energy protons. The reference beam consisted of Cs-137 gamma rays (Toshiba gamma cell RS-G-50) with a dose rate of approximately 1.6 Gy/min at a focus skin distance of 21 cm [6]. Thimble ionization chambers were used for measuring Cs-137 gamma rays. Groups of five mice were anesthetized with pentobarbital (50 mg/kg), immobilized by taping their right hind legs on a Lucite plate and legs placed within a 28 × 100 mm rectangular field for carbon ions. A doughnut-shaped radiation field with a 30-mm rim was used to collimate a vertical beam of gamma rays. We put a small round block in the center of a large circle on a 10-mm thick plate of polymethyl methacrylate (PMMA), which made the radiation field. The block and circle were made of 5-cm thick lead. The length of legs irradiated with carbon ions was therefore 2 mm shorter than that with gamma rays (30 mm minus 28 mm) [6].

Skin contraction

We employed the tattooing method to quantitate skin contraction in irradiated leg skin [9–11]. Briefly, hairs on the right hind leg of a mouse were removed by applying a depilatory agent, and two tattoo spots separated by approximately 18 mm distance were made into the outer leg skin by using a commercially available tattoo machine and Indian ink 3–7 days before irradiation. Calipers were used to measure the distance between the two tattoo spots once a month until the end of the study. The post-irradiation distance (a) was compared to that for pre-irradiation (b), and percent skin contraction was calculated by a formula (b-a)/b × 100. This method is used by us [12] and another group [13] as an experimental model for cutaneous radiation-induced fibrosis. Variation in measurement days was 8 (range:2–26) days.

Data acquisition and analysis

The spot distance was measured approximately once a month for one year. As measurement days varied among experiments, we used averaged days for all radiation schemes. Each radiation scheme consisted of corresponding LET and number of fractions and contained approximately 50 mice. Dose–response for each scheme was obtained by applying a cubic function and calculating a radiation dose to induce 30% skin contraction (Fig. 1). The data for each dose–response curve was fitted to a cubic polynomial function using the least-squares method. A 95% confidence limit at 30% contraction was calculated using Mahalanobis distance which we use also for skin reaction and tumor growth delay [13–15].

RBE of carbon ion beams was calculated by two different methods. One was to compare equieffective doses between carbon ions and reference gamma rays for each fractionation scheme. In another method, survival parameter alpha which was calculated by applying Fe-plot to equieffective doses of multiple fractionation schemes were compared between carbon ions and gamma rays. RBE values obtained by the second method were used to study the change of biological doses within the SOBP after irradiation.

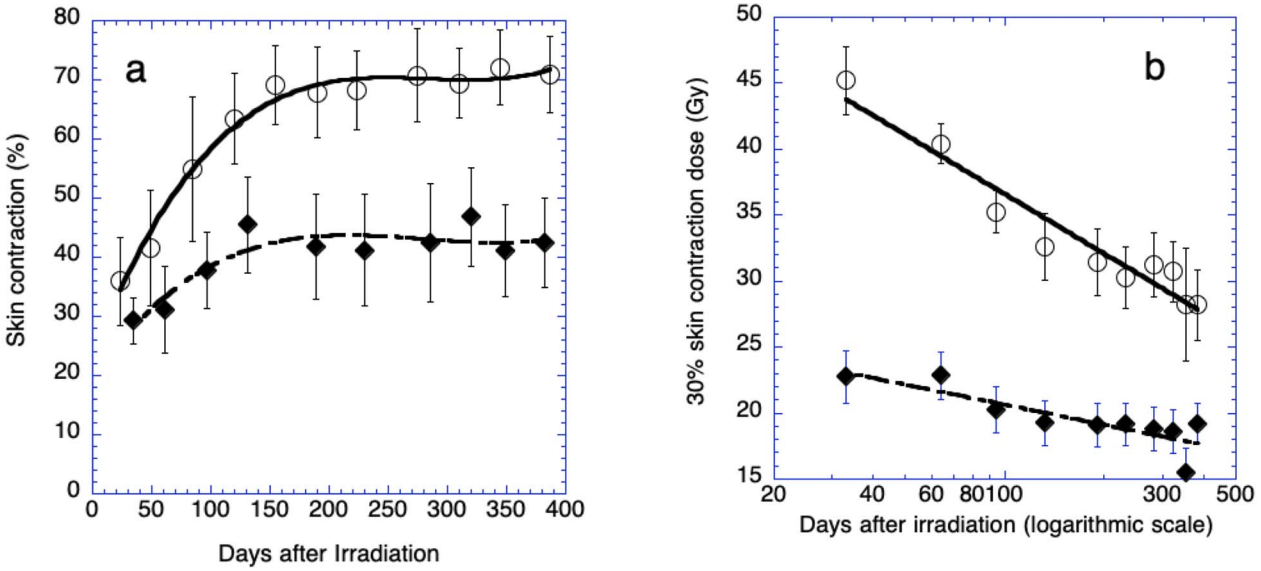

Fig. 2. Time course of skin contraction after single doses. (a) Skin contraction after 45 Gy of gamma rays (◯) or 22 Gy of 100 keV/μm carbon ions (◆). Symbols and bars are mean and standard deviation. (b) Daily reduction of the equieffective dose for 30% skin contraction. It should be noted that the horizontal axis is a logarithmic scale. Gamma rays (◯), 100 keV/μm carbon ions (◆). Mean and 95% confidence limit.

The raw data of the inter-spot distance can be downloaded as http://dx.doi.org/10.17632/8bv33rzpnf.1 (Excel book).

RESULTS

Typical dose responses of skin contraction after single doses of gamma-rays and 100 keV/μm carbon-ions are shown in Fig. 1. Gamma rays produced sigmoid-like dose responses with a saturation level of 50∼75%, contraction depending on days after irradiation. On the other hand, carbon ions resulted also non-linear but overkill dose–responses with a peak level of 40∼60% contraction.

Time courses of skin contraction after single doses with these LETs were compared with each other (Fig. 2a). In this specific comparison, doses were selected that induced similar contraction at the initial measurement of 32 days. The two curves clearly show the progression of skin contraction up to ∼121 days after irradiation followed by less prominent/saturated progression thereafter up to 380 days. An equieffective dose inducing 30% skin contraction after a single fraction was calculated for each LET and plotted against days after irradiation (Fig. 2b). Equieffective doses were highest at Day 33 and decreased with the time to which the logarithmic scale was applied. This decrease was observed for all fractionation schemes and possessed slopes similar to each other. The steepness of the slope means the progression speed of skin contraction so that the steeper the slope more rapid the progression. When the slopes of the decrease for each LET were averaged, the slope of this logarithmical decrease also declined with LET (Fig. 3). This means that the progression of skin contraction depends on LET and is less prominent for higher LET radiation.

RBE values for various LETs were calculated by comparing the equieffective doses between carbon ions and reference Cs-137 gamma rays (Fig. 4). In a single fraction, RBE values at Day 33 ranged between 1.40 and 2.11, depending on LET. This range was similar for Day 384 but slightly wider, i.e. 1.63∼3.47. This similarity of RBE values between early and late days after irradiation was also observed for fractionated doses, even though RBE values were larger than those for single doses.

One issue is whether the RBE values change with days after irradiation was studied by applying linear regression analysis. The null hypothesis was rejected when p values were larger than 0.05, and the slope was judged as zero. Within a total of 48 radiation schemes studied, 23 schemes did not show significant changes of RBE between day 33 and day 384. However, 21 schemes showed rather significant increases. Only four schemes decreased with time (Table 1). These data indicate that the RBE of carbon ions either increases or is stable after irradiation with a few exceptions.

RBE was also calculated by comparing survival parameters between carbon ions and gamma rays. Reciprocal total doses of 1 through 8 fractions were plotted against dose per fraction (Fig. 5). Two parameters of alpha and beta were calculated by Fe-plot analysis [16]. Dependence of these parameters on days after irradiation was observed for alpha, but not for beta nor α/β ratio. Alpha values were relatively stable with time for low LET beams but increased for higher LET (Fig. 6a). Meanwhile, beta values did not show any constant characteristic: intermediate LET beams showed prominent change with time while RBE of 100 keV/μm carbon beams was rather stable (Fig. 6b). Resultant α/β ratios showed huge variations for higher LET beams (Fig. 6c). When plotted against LET, alpha increased any time after irradiation, and this increase was most prominent for the latest time of observation, i.e. Day 384 (Fig. 7a). RBE values calculated by comparing alpha between carbon ions and gamma rays also increase with LET (Fig. 7b). This increase was again most prominent for the latest time of observation.

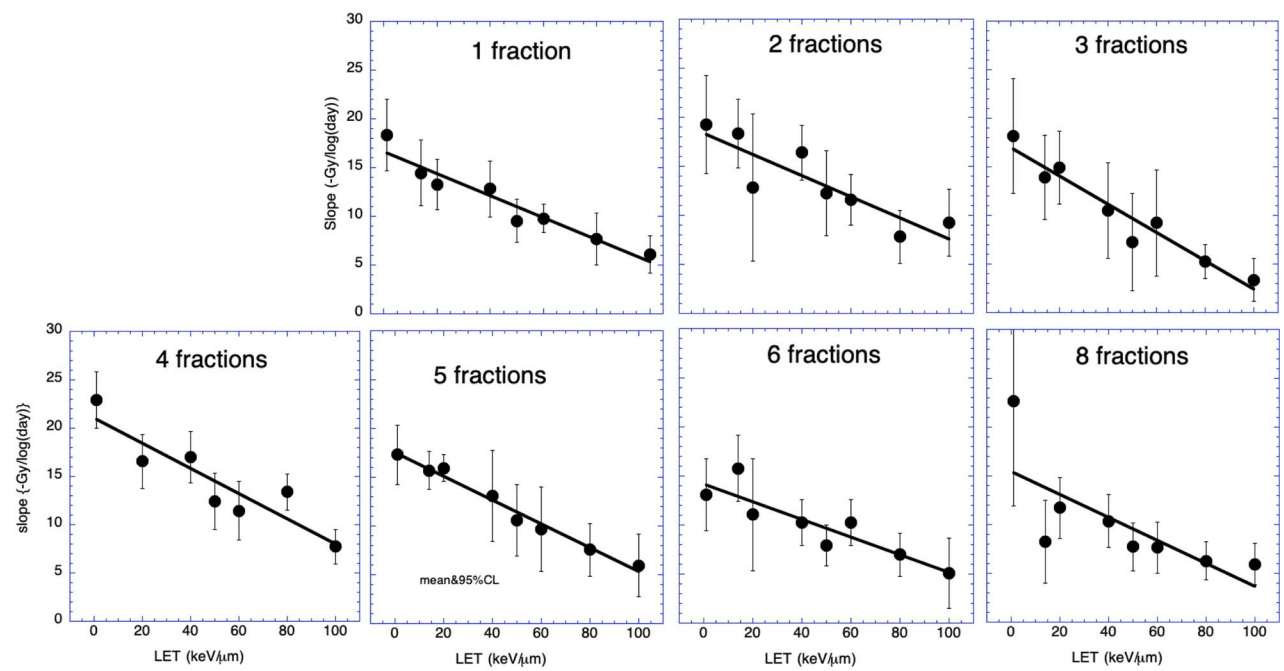

Fig. 3. The logarithmic decrease of the equieffective dose against LET for multifaction schemes. The slopes of the daily reduction for other LETs were also calculated and plotted against LET. The slopes of the daily reduction for single and multifaction schemes were averaged to calculate mean values and plotted against LET. Bars are 95% confidence limit. Slopes of regression lines (i.e. daily-dose reduction/LET) shown in each panel are −0.098, −0.108, −0.145, −0.131, −0.122, −0.091, −0.118 for 1, 2, 3, 4, 5, 6 and 8 fractions, respectively.

Table 1. Slopes of regression lines in Fig. 3. The slope of each line was analyzed for all radiation schemes and whether RBE changed with days was studied. When p values of linear regression exceeded 0.05, slopes were judged as either increase (red) or decrease (blue) depending on the plus or minus sign. Judgment of no change (white) was for p values smaller than 0.05

LET (keV/μm)	Number of fractions						
	1	2	3	4	5	6	8
14	increase	increase	no change		increase	increase	decrease
20	no change	no change	increase	increase	increase	no change	no change
40	increase	increase	no change	increase	increase	increase	no change
50	no change	increase	no change	increase	increase	increase	no change
60	no change	no change	increase	increase	no change	increase	no change
80	no change	no change	decrease	increase	no change	increase	no change
100	decrease	no change	decrease	no change	no change	no change	no change

Whether the flatness of biological dose distribution within the SOBP design based on *in vitro* cell kill is also valid for late skin contraction. This was answered here by comparing biological doses between various days after irradiation (Fig. 8). The biological dose calculated here has no dimension. A method reported by Kanai *et al.* [17] was modified and employed here to calculate biological dose. In brief, a physical dose at given position within a SOBP is relative to the dose normalized to 1 at the center of the SOBP. As physical dose has no dimension, biological dose also has no dimension. The biological dose was calculated by multiplying: (i) physical dose relative to the center, and (ii) RBE at a given depth of interest within the SOBP. RBE values used here are identical to those shown in Fig. 5b. Biological doses at Day 33 ranged from 2.63 to 2.90 and were approximately the same as the doses for 10% survival of HSG cell kill [2, 3, 6] and were distributed flat within the 6-cm SOBP. One year after irradiation, biological doses increased up to 3.82 (range 3.36–4.36) at Day384 but distribution remained flat. The flatness of the distribution was analyzed by studying the slopes of the regression lines for 5 positions

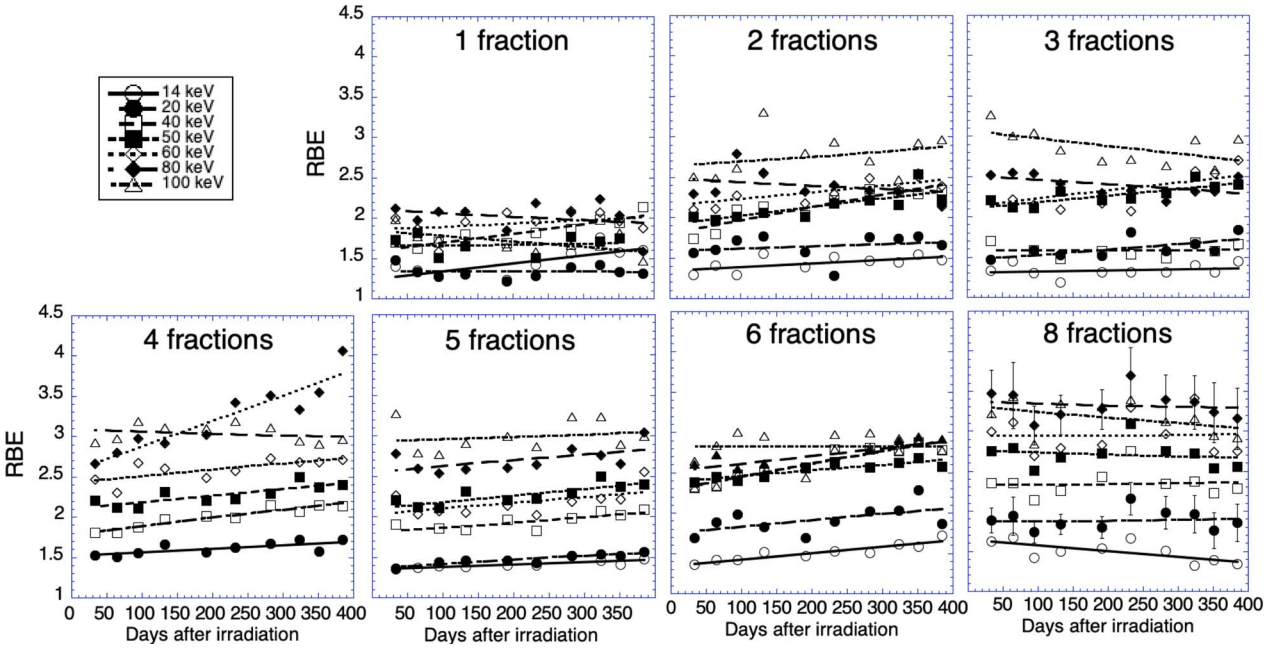

Fig. 4. Change of RBE after single and fractionated irradiation irradiations. RBE was calculated by comparing equieffective doses between reference gamma rays and carbon ions and plotted against days after irradiation. Symbols are mean values for carbon ions of; 14 keV/μm (open circle), 20 keV/μm (closed circle), 40 keV/μm (open square), 50 keV/μm (closed square), 60 keV/μm (open diamond), 80 keV/μm (closed diamond), and 100 keV/μm (open triangle).

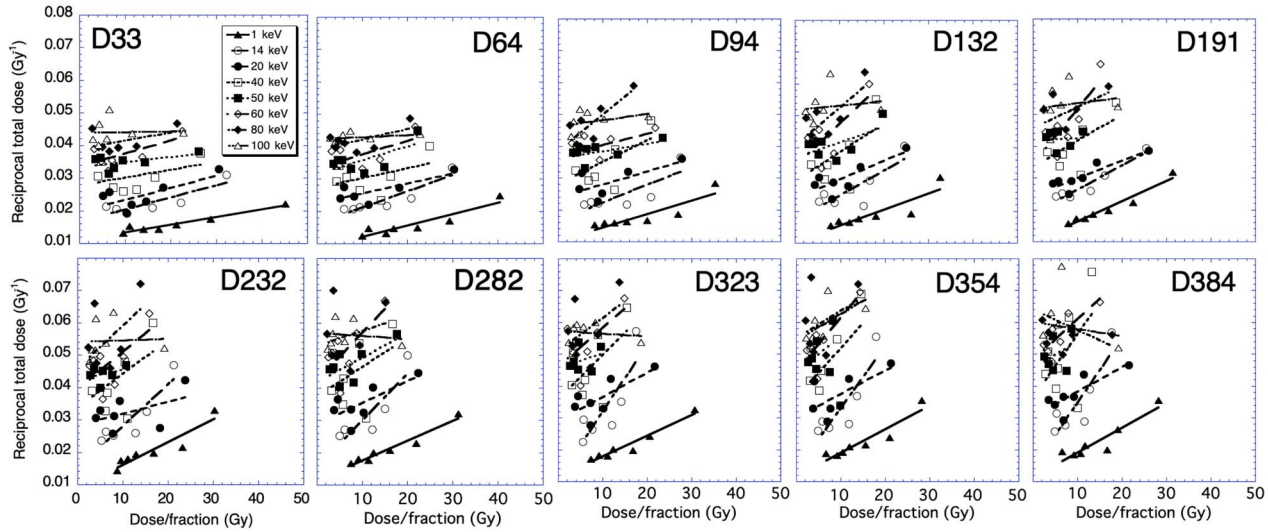

Fig. 5. Fe-plot for skin contraction. Equieffective doses of 30% skin contraction were obtained for 1 through 8 fractions and used to calculate alpha and beta values using Fe-plot. Symbols are: 1 keV/μm (closed triangle), 14 keV/μm (open circle), 20 keV/μm (closed circle), 40 keV/μm (open square), 50 keV/μm (closed square), 60 keV/μm (open diamond), 80 keV/μm (closed diamond) and 100 keV/μm (closed triangle). A value on Y-axis at dose zero extrapolated from the linear regression line is alpha / E while its slope is beta/E.

within the SOBP. The null hypothesis was rejected when p values were larger than 0.05, and the slope was judged as zero. The mean, standard error of the mean is summarized in Table 2 along with p values to judge the null hypothesis. None of the slopes are significantly different from zero, meaning the distribution is flat for all SOBPs studied.

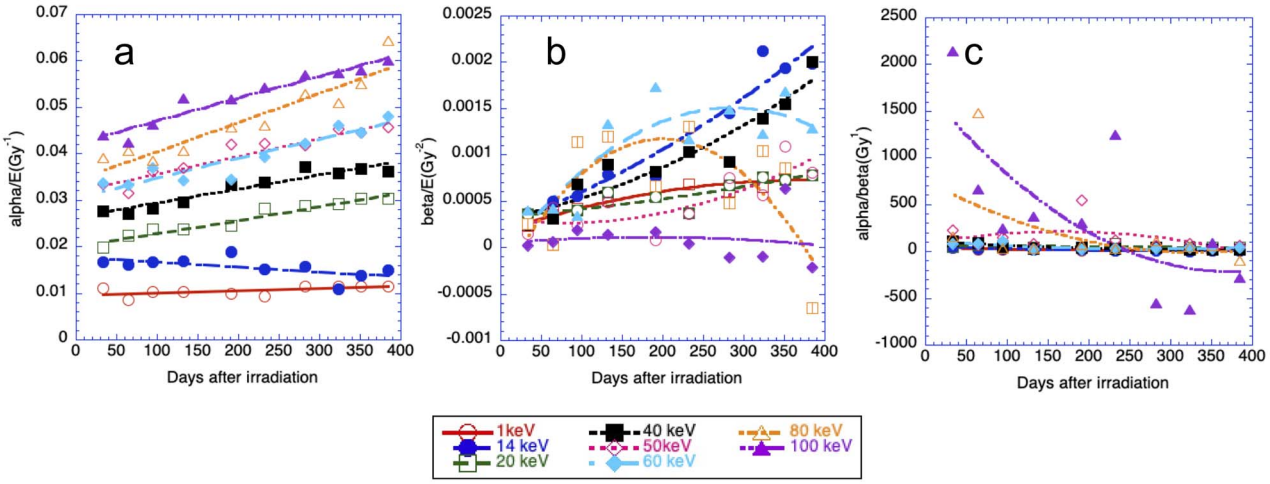

Fig. 6. Dependence of survival parameters on time after irradiation. Survival parameters were calculated from Fe-plots shown in Fig. 5 and plotted against days after irradiation. (a) alpha/E, (b) beta/E, and (c) alpha/beta. Symbols are: 1 keV/μm (open circle), 14 keV/μm (closed circle), 20 keV/μm (open square), 40 keV/μm (closed square), 50 keV/μm (open diamond), 60 keV/μm (closed diamond), 80 keV/μm (open triangle), 100 keV/μm (closed triangle).

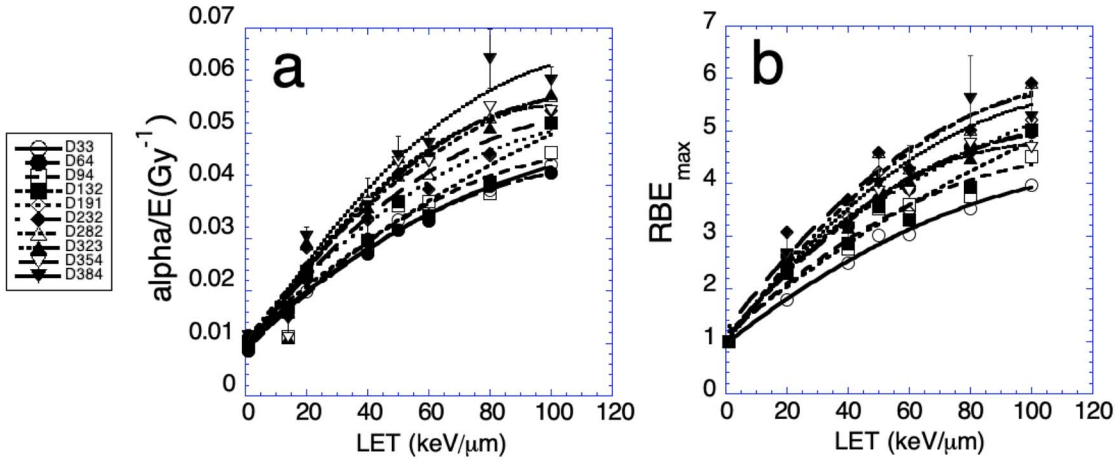

Fig. 7. Dependence of alpha and RBE$_{max}$ on LET. (a) Alpha/E at various days after irradiation was calculated for each LET. (b) RBE$_{max}$ of carbon ions was calculated by comparing alpha/E of carbon ions to that of gamma rays. Symbols are Day 33 (open circle), Day 64 (closed circle), Day 94 (open square), Day 132 (closed square), Day 191 (open diamond), Day 232 (closed diamond), Day 282 (open triangle), Day 323 (closed triangle), Day 354 (open inverted triangle), Day 384 (closed inverted triangle). Symbol and bar are mean and sem.

DISCUSSION

We report two facts that have never been reported in published literature: radiation dermal fibrosis progressed less for high LET carbon ions than photon and biological dose distribution for dermal fibrosis within the SOBP was still flat 1 year after carbon-ion radiation.

Time-dependence for RBE of carbon ions

Time-dependent increase of RBE was observed by directly comparing equieffective doses (Fig. 4, Table 1) and more clearly by comparing survival parameter alpha (Fig. 7b). This increase is due to a different rate of progression for skin contraction between gamma rays and carbon ions. Dose responses of carbon ions shifted to the left of gamma rays irrespective of time after irradiation (Fig. 1). When plotted against time after irradiation, the rate of 30% skin contracture from equieffective doses of gamma rays progressed more rapidly than for carbon ions (Fig. 2b). This means skin contraction progressed more quickly after gamma rays than carbon ions which agreed with the time-dependent change of percent skin contraction (Fig. 2a). The rate of progression (i.e. the reduction speed of equieffective doses) is inversely related to LET so that the higher the LET slower the progression (Fig. 3). The LET-dependent decrease of progression is equally observed for any

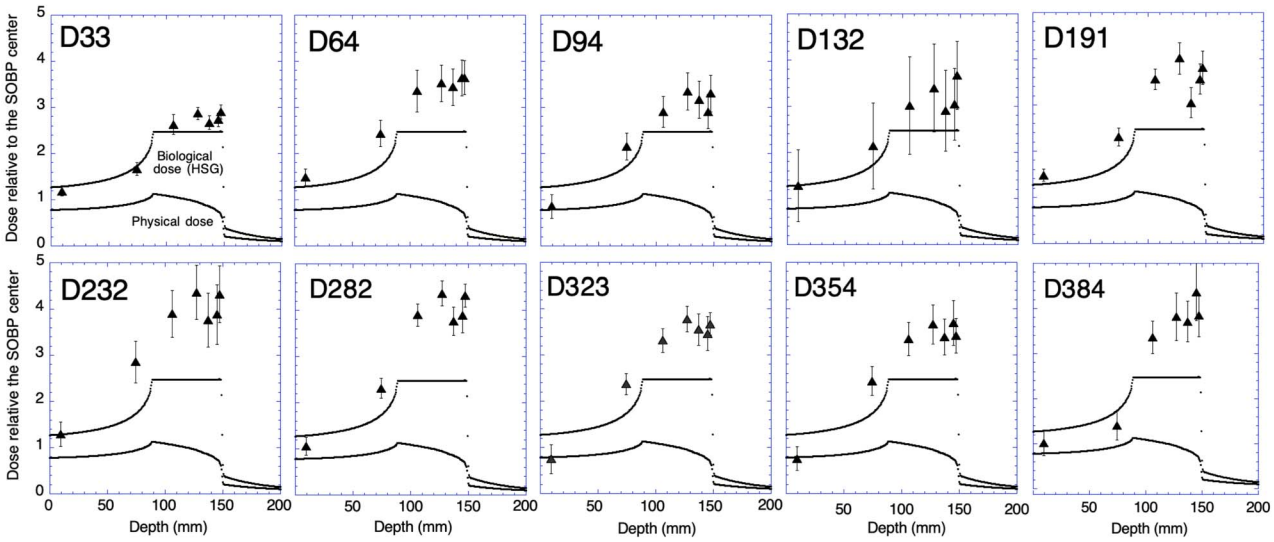

Fig. 8. Biological dose distribution within the SOBP. RBE_{max} was used to calculate a biological dose at a given depth along with the 6-cm SOBP. LET of two entrance positions are 14 keV/μm and 20 keV/μm whereas the rest of the five positions are for 40, 50, 60, 80 and 100 keV/μm, respectively. Mean and SEM. Upper- and lower curves are respectively biological dose calculated for 10% survival of HSG cells and physical dose.

Table 2. The flatness of biological dose distribution within the SOBP. Excluding two entrance positions, five positions within the SOBP in Fig. 8 were studied for flatness of biological dose distribution. The slope of the regression line has a unit of dose/mm p values smaller than 0.05 were considered significant

slope	Days after irradiation									
	32	64	94	132	191	232	282	323	354	384
mean	0.00381	0.00641	0.00431	0.00688	−0.00058	0.00287	0.00292	0.00517	0.00358	0.01694
standard error	0.00354	0.00215	0.00678	0.01016	0.01239	0.00932	0.00486	0.00544	0.00519	0.00768
p value	0.36	0.06	0.57	0.55	0.97	0.78	0.59	0.41	0.54	0.11

fractionation schemes. This means that LET is a major determinant for skin contraction and suggests that the repair mechanisms commonly associated with radiation cell kill including DNA repair and tissue repopulation may not be responsible for the progression of skin contraction.

Why does the skin contraction after gamma rays progress more rapidly and prominently than carbon ions? As clearly shown in Fig. 3, skin contraction strongly depends on LET. High LET radiation is known to cause clustered and complex damage [18] which results in stronger cell kill than photons. Fibroblasts surviving high LET radiation may carry this damage and respond differently than do cells surviving simple damage do. The difference of damage between high and low LET radiation should also have affected cells/tissues surrounding skin, which may result in different production of pro-fibrosis cytokines. Fibrosis is a dose-limiting complication that emerges late after radiotherapy. Unlike early effects that are transient and settle after a few weeks, late effects tend to be irreversible and even progressive in severity [19]. In response to fibrogenic cytokines released by inflammatory and other cell types, fibroblasts differentiate into myofibroblasts which are commonly found in pathological tissues like hypertrophic scarring [20]. Local fibroblasts are not the only sources of myofibroblasts given that epithelial, endothelial and smooth muscle cells are alternative progenitors. No report could be found for late effects of carbon ions on skin contraction or dermal fibrosis. Oxidative stress caused in cultured human fibroblasts is compared between carbon ions and X-rays in such that, at Day 7, the production of superoxide dismutase (SOD) is higher for X-rays than carbon ions while that of IL-6 is higher for carbon ions than X-rays [21]. They report no data beyond one month.

LET and volume effect

Carbon ion beams in the present study have limited depth distribution so that the dose delivered to the skin by carbon ion beams with

100 keV/μm should have been reduced to half when they reached the knee bone and cannot deliver the same LET to the entire irradiated legs. We have observed irradiated mice showing severe skin contraction but not leg contracture after 100 keV/μm carbon ion beams while mice irradiated with lower LET, and therefore deeper penetration beams show clear leg contracture (data not shown). As volume effect is inevitably associated with 100 keV/μm carbon ion beams in the present study, we here also used lower LET beams which can penetrate legs and therefore minimize the volume effect from data interpretation.

Unique time dependences for beams are observed in Fig. 6b and c. Beta values of 60 and 80 keV/μm initially increase with time and later decrease. Alpha/beta ratios decrease with time for 80 and 100 keV/μm. No report is found to explain this unique time dependence. As the volume irradiated with higher LET beams is smaller than that with lower LET beams, the smaller volume of higher LET radiation may affect the dose–response of skin contraction. It is however difficult to explain the complex kinetics of the beta and the alpha/beta ratio.

Choice of endpoint

The method we employed here to quantitate dermal fibrosis was first reported by Hayashi in the 1970s [9], followed by Masuda *et al.* [10] and Stone [11]. They also locally irradiated the hind legs of mice with Cs-137 gamma rays and measured the tattoo spot's distance of both the treated and control hind legs for up to one year. Stone compares leg contracture and skin contraction, reporting that the two assays measure the same phenomena of late radiation responses. We also report that skin contraction in mice 1 year after gamma-ray radiation correlates well to leg contracture [12]. Histological observation of irradiated skin shows hyperplasia of the epidermis and thickening of the dermis, suggesting that dermal fibrosis is closely related to skin contraction. Similarly, Horton *et al.* [13] observed histologically that skin thickness and collagen content parallelly increased 150 days after 35 Gy X-ray radiation in mouse hind limb. We used the endpoint of skin contraction instead of leg contracture in the present study because unlike photon, LET of carbon ions changes along with beam path. The thickness of leg skin in C3H mice used in the present study was ~90 μm while that of muscle was more than 5 mm; therefore, the variation of LET for skin was narrower than that for underlying muscle/knee. Leg contracture is caused by not only skin contraction but also damage to the muscle/knee joint [12]. Whether housing conditions could influence skin contraction is not known.

Another method to measure radiation fibrosis in mice is reported for carbon ion beams [22]. Zhou *et al.* use CT to invent a fibrosis index that is calculated from lung tissue density measured by the Hounsfield unit. They report RBE values and survival parameters of α/β ratios, but do not show time-course change for lung fibrosis. How this CT method relates to other methods like ours is not known yet.

Difference between RBE and RBE_{max}

RBE values in Fig. 4 are for individual fractionation but those in Fig. 7b (i.e. RBE_{max}) are for collective fractionation. As stated in Materials and Methods, RBE values of carbon ions relative to gamma rays were obtained by comparing between carbon ions and gamma rays either: (i) directly equieffective doses, or (ii) survival parameters calculated using Fe-plot analysis. RBE thus obtained could be named here either simple RBE or RBE max for the former (1) or the latter (2), respectively. As shown in Fig. 4 and Table 1, RBE of most radiation schemes either increased or stayed unchanged after irradiation. On the other hand, alpha values necessary to calculate RBE_{max} are obtained by using various fractionation schemes but could not be calculated for individual fractionation schemes. As the two methods are different, resultant RBE values are different even though both methods use equieffective doses for calculation. RBE_{max} uses the parameter alpha that applies to small doses whereas the doses producing 30% skin contraction are as large as 30~40 Gy of gamma rays (Fig. 1). We can assume that RBE for small doses is larger than that for large doses due to shouldered dose–response.

RBE of carbon ions for other late responding tissues

Karger *et al.* report that RBEs for 13 keV/μm and 125 keV/μm carbon ions (SOBP) are respectively 1.44 and 1.77 after single-dose exposure to rat spinal cord causing paralysis [23]. Zhou *et al.* [22] report that lung fibrosis developed in mice after receiving thoracic irradiation with 86 keV/μm carbon ions (SOBP) as measured 24 weeks later by quantitative CT imaging. Using a unique endpoint of the fibrosis index, they report that RBE of carbon ions after 5 fractions depends on fraction size and ranges between 1.82 and 4.26. RBE of carbon ions in the present study corresponding to Zhou's radiation scheme of 5 fractions of 80 keV/μm at Day 191 was 2.6 ± 0.27 (Fig. 3) and was within the RBE range they reported.

Time-dependent change of RBE has never been reported for other tissues.

LQ model

The classical framework for discussing early and late side effects was the target-cell hypothesis: that severity of side effects mainly reflected cell depletion as a result of the direct cell killing of a putative target cell leading to subsequent functional deficiency. This was the prevailing biological model until the mid-1990s [18]. In the present study, Fe-plot analysis described fibrosis development only in part so that RBE and alpha term showed a clear dependence on LET (Fig. 6a, Fig. 7a) while beta term and α/β ratio did not (Fig. 6b–c). The reason why dose interaction is not involved in the development could simply be explained by knowing that cell kill is not responsible for fibrosis. Radiosensitivity of fibroblasts does not relate to fibrosis development in mice and humans [24, 25]. As fibrosis development is caused by any response of survived cells to radiation, any new model incorporating survived cell-response should be developed in the future.

ACKNOWLEDGEMENTS

We appreciate Drs. Howard Thames and Helen B. Stone of helpful discussions and useful suggestions. This work was supported by Research Project with Heavy Ions at QST-HIMAC.

REFERENCES

1. Statistics of patients treated in particle therapy facilities worldwide: https://www.ptcog.ch/index.php/ptcog-patient-statistics

2. Kanai T, Endo M, Minohara S et al. Biophysical characteristics of HIMAC clinical irradiation system for heavy-ion radiation therapy. *Int J Radiat Oncol Biol Phys* 1999;44:201–10.
3. Matsufuji N, Kanai T, Kanematsu N et al. Specification of carbon ion dose at the National Institute of Radiological Sciences (NIRS). *J Radiat Res* 2007;48 Suppl A:A81–6.
4. Krämer M, Scholz M. Treatment planning for heavy-ion radiotherapy: calculation and optimization of biologically effective dose. *Phys Med Biol* 2000;45:3319–30.
5. Karger CP, Peschke P. RBE and related modeling in carbon-ion therapy. *Phys Med Biol* 2018;63:1–35.
6. Uzawa A, Ando K, Kase Y et al. Designing a ridge filter based on a mouse foot skin reaction to spread out Bragg-peaks for carbon-ion radiotherapy. *Radiother Oncol* 2015;115:279–83.
7. Choi YW, Munden RF, Erasmus JJ et al. Effects of radiation therapy on the lung: radiologic appearances and differential diagnosis. *Radiographics* 2004;24:985–97.
8. Citrin DE, Prasanna Pataje GS, Walker AJ et al. Radiation-induced fibrosis: mechanisms and opportunities to mitigate. Report of an NCI workshop, September 19, 2016. *Radiat Res* 2017;188:1–20.
9. Hayashi S, Herman DS. Effect of fractionation of radiation dose on skin contraction and skin reaction of Swiss mice. *Radiology* 1972;103:431–7.
10. Masuda K, Hunter N, Withers HR. Late effect in mouse skin following single and multifractionated irradiation. *Int J Radiation Oncology Biol Phys* 1980;6:1053–61.
11. Stone H. Leg contracture in mice: an assay of normal tissue response. *Int. J. Radiation Oncology Biol. Phys.* 1984;10:1053–61.
12. S Matsushita 1, K Ando, S Koike et al. Radioprotection by WR-151327 against the late normal tissue damage in mouse hind legs from gamma ray radiation. *Int J Radiat Oncol Biol Phys* 1994;30:867–72.
13. Horton JA, Hudak KE, Chung EJ et al. Mesenchymal stem cells inhibit cutaneous radiation-induced fibrosis by suppressing chronic inflammation. *Stem Cells* 2013;31:2231–41.
14. Ando K, Koike S, Nojima K et al. Mouse skin reactions following fractionated irradiation with carbon ions. *Int J Radiat Biol* 1998;74:129–38.
15. Yoshida Y, Ando K, Ando K et al. Evaluation of therapeutic gain for fractionated carbon-ion radiotherapy using the tumor growth delay and crypt survival assays. *Radiother Oncol* 2015;117:351–7.
16. Douglas BG, Fowler JF. The effect of multiple small doses of X-rays on skin reactions. In the mouse and a basic interpretation. *Radiat Res* 2012;66:401–20.
17. Kanai T, Furusawa Y, Fukutsu K et al. Irradiation of mixed beam and Design of Spread-out Bragg Peak for heavy-ion radiotherapy. *Radiat Res* 1997;147:78–85.
18. Hada M, Georgakilas AG. Formation of clustered DNA damage after high-LET irradiation: a review. *J Radiat Res* 2008;49:203–10.
19. Bentzen SM. Preventing or reducing late side effects of radiation therapy: radiobiology meets molecular pathology. *Nat Rev Cancer* 2006;6:702–13.
20. Shirakami E, Yamakawa S, Hayashi K. Strategies to prevent hypertrophic scar formation: a review of therapeutic interventions based on molecular evidence. *Burns & Trauma* 2020;8:1–7.
21. Laurent C, Leduc A, Pottier I et al. Dramatic increase in oxidative stress in carbon- irradiated normal human skin fibroblasts. *PLoS One* 2013;8:1–10.
22. Zhou C, Jones B, Moustafa M et al. Determining. RBE for development of lung fibrosis induced by fractionated irradiation with carbon ions utilizing fibrosis index and high-LET BED model. *Clinical and Translational Radiation Oncology* 2019;14:25–32.
23. Karger CP, Reschke P, Sanchez-Brandelik R et al. Radiation tolerance of the rat spinal cord after 6 and 18 fractions of photons and carbon ions: experimental results and clinical implications. *Int J Radiation Oncology Biol Phys* 2006;66:1488–97.
24. Christine L, Dileto CL, Travis EL. Fibroblast radiosensitivity in vitro and lung fibrosis in vivo: comparison between a fibrosis-prone and fibrosis-resistant mouse strain. *RadiatRes* 1996;146:61–7.
25. Russel NS, Grummels A, Hart AA et al. Low predictive value of intrinsic fibroblast radiosensitivity for fibrosis development following radiotherapy for breast cancer. *Int J Radiat Biol* 1998;73:661–70.